nature photonics

LETTERS

PUBLISHED ONLINE: 2 MARCH 2014 | DOI: 10.1038/NPHOTON.2014.40

Two-plasmon quantum interference

James S. Fakonas[1,2], Hyunseok Lee[2], Yousif A. Kelaita[2] and Harry A. Atwater[1,2]*

Surface plasma waves on metals arise from the collective oscillation of many free electrons in unison. These waves are usually quantized by direct analogy to electromagnetic fields in free space[1–3], with the surface plasmon, the quantum of the surface plasma wave, playing the same role as the photon. It follows that surface plasmons should exhibit all the same quantum phenomena that photons do. Here, we report a plasmonic version of the Hong–Ou–Mandel experiment[4], in which we observe unambiguous two-photon quantum interference between plasmons, confirming that surface plasmons faithfully reproduce this effect with the same visibility and mutual coherence time, to within measurement error, as in the photonic case. These properties are important if plasmonic devices are to be employed in quantum information applications[5], which typically require indistinguishable particles.

The close analogy between the photon and the surface plasmon in quantum theory has invited experimental tests. Experiments to date have confirmed that surface plasmons do indeed exhibit many familiar quantum phenomena, demonstrating, for example, the preservation of single-photon statistics[6–9] and entanglement[10,11] upon exciting surface plasma waves with non-classical light. Other studies report that it is possible to prepare superposed[12] and squeezed[13] states of the plasmon field. In these experiments, strong dispersion and dephasing in plasmonic systems, absent in most free-space experiments, do not appear to degrade the visibility of these quantum effects.

Two-photon quantum interference (TPQI) represents another opportunity to study the quantum mechanics of surface plasmons. In typical experiments with free-space optics or dielectric waveguides[14], pairs of indistinguishable photons enter the inputs of a 50–50 splitting element that mixes their paths. The splitter imparts a π phase shift, required by energy conservation in the lossless case[15], to the state in which both photons are reflected relative to that in which both photons are transmitted. If these two states are identical, which is to say in our experiment and in most others that the photons are indistinguishable, then this π phase difference causes them to cancel exactly, leaving a superposition of states in which both photons are found together in one or the other of the two outputs, but never in each output separately. Accordingly, detectors placed at the two outputs never click simultaneously. A typical measurement consists in delaying the arrival of one photon at the splitter by a variable amount and measuring coincidence counts at the outputs: when the relative delay is larger than the mutual coherence time of the photons, the detectors record a baseline rate of simultaneous counts C_{base}, but when the delay is set so that the photons arrive simultaneously this rate drops to a minimum C_{min} due to TPQI. The visibility of interference, defined as $1 - C_{min}/C_{base}$, must be less than 0.5 for classical light[16], but is usually near unity in quantum experiments[4,14].

Importantly, to observe high-visibility TPQI in a plasmonic system requires not only that the plasmonic components preserve the non-classical statistics of the input light, but also that the resulting biphoton states retain their mutual coherence. In our experiment, this criterion corresponds to both photons remaining indistinguishable as they convert to plasmons and interfere. Recent experiments with plasmonic thin-film structures[17,18] and weakly confined long-range surface plasmons[19] suggest that conversion to and from a plasmonic mode does not necessarily render a photon distinguishable from an initially indistinguishable partner. Nevertheless, small reductions in the visibility of TPQI did occur and were attributed to distortions of the single-photon wave packets[17] and unbalanced dispersion[19]. Moreover, a very recent experiment[20] reports TPQI in strongly confining plasmonic waveguides but with reduced visibility compared to the case of a dielectric 50–50 coupler. Our measurement sheds light on these results and provides definitive evidence of plasmonic quantum interference.

Figure 1 presents a schematic of our experiment. We used a semiconductor diode laser and a nonlinear crystal to create degenerate pairs of single photons by spontaneous parametric downconversion (SPDC), which we collected into optical fibres. After one photon traversed a fibre-coupled adjustable delay line, both were coupled back into free-space beams and focused through a microscope objective into the ends of dielectric waveguides fabricated on a silicon chip. At the output side of the chip, lensed multimode fibres collected light out of the waveguides and sent it to our single photon avalanche photodiodes (SPADs). To improve the efficiency of coupling into and out of the waveguides, we patterned polymethyl methacrylate (PMMA) spot-size converters[21] over their ends. With this design, we typically observed 30–35% transmission through waveguides with no plasmonic components.

Following the approach of Briggs and colleagues[22], we integrated dielectric-loaded surface plasmon polariton waveguides (DLSPPWs) directly into our dielectric waveguides, as shown in Fig. 2a. We fabricated these chips with a combination of electron-beam lithography, plasma etching and metal deposition techniques (see Methods), using silicon nitride for the dielectric waveguides and PMMA on gold for the DLSPPWs. A 500 μm S-bend in each dielectric waveguide (Fig. 2b) ensured that any stray light that was not fully coupled into the dielectric waveguides at their inputs did not reach the lensed fibres at the outputs. The dielectric and plasmonic waveguides each supported a single vertically polarized mode, which we calculated with a finite-difference frequency-domain mode solver (Fig. 2c). We also calculated a dispersion plot for the DLSPPWs (Fig. 2d) to confirm that our operating wavelength, 814 nm, was far from the cut-on wavelength for the second-order mode. From measurements of transmission through DLSPPWs of different lengths (Supplementary Section 3), we estimated the 1/e decay length of the plasmonic mode to be $\sim$6.8 μm and the coupling efficiency between the dielectric and plasmonic waveguides to be $\sim$0.66 per transition.

As a reference, we first measured TPQI in a dielectric 50–50 directional coupler made from silicon nitride waveguides, observing a visibility of 0.944 ± 0.003. The data, normalized for direct

[1]Kavli Nanoscience Institute, California Institute of Technology, Pasadena, California 91125, USA, [2]Thomas J. Watson Laboratories of Applied Physics, California Institute of Technology, Pasadena, California 91125, USA. *e-mail: haa@caltech.edu

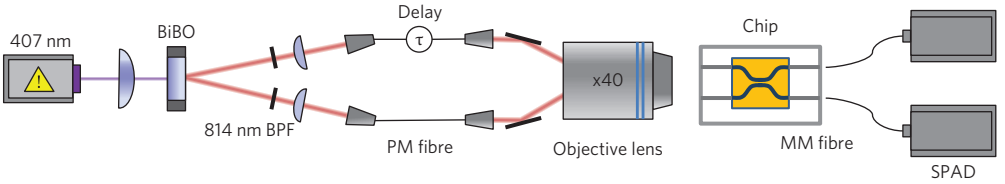

Figure 1 | Schematic of the TPQI measurement. A 407 nm diode laser and a bismuth borate (BiBO) crystal aligned for SPDC generate pairs of single photons at 814 nm. The photons pass through band-pass filters (BPF) and enter polarization-maintaining (PM) fibres, where one is delayed by an adjustable amount. A second pair of collimators couples the photons back into free space and a ×40 microscope objective focuses them into separate waveguides on a photonic chip. At the outputs of the chip, multimode (MM) optical fibres collect the photons and send them to SPAD detectors.

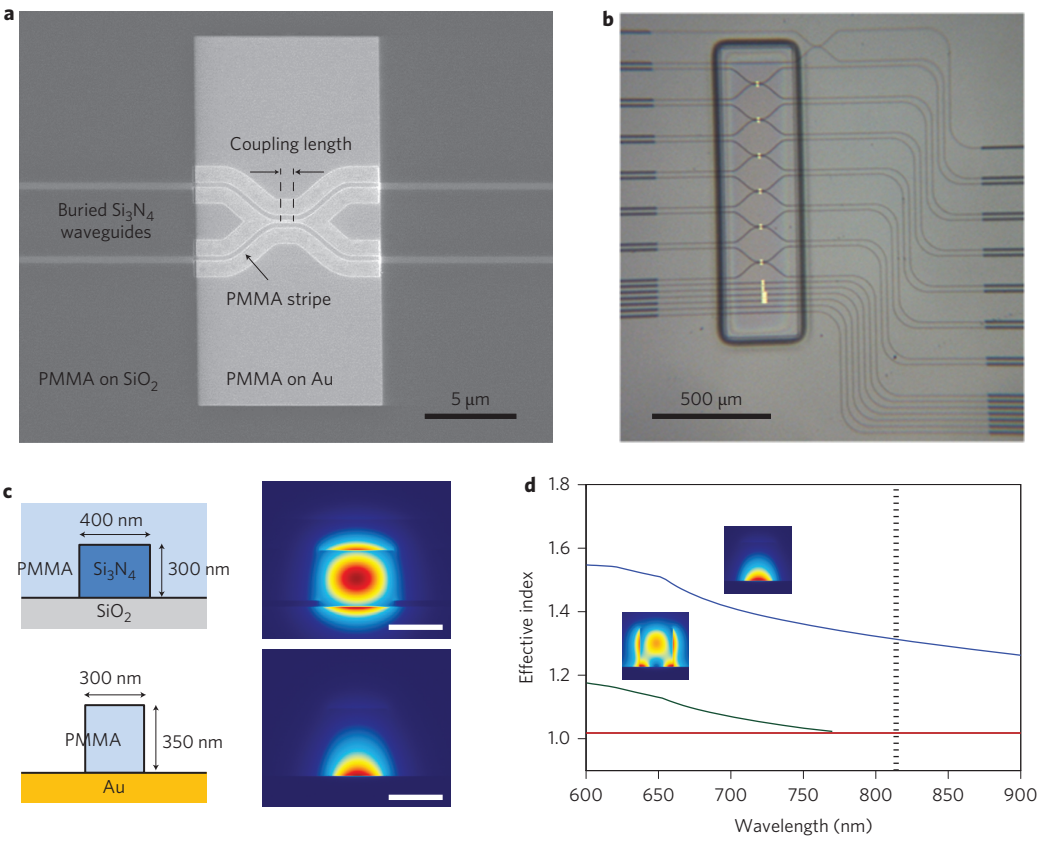

Figure 2 | Design of the waveguides. a, Silicon nitride waveguides deliver pairs of photons to a directional coupler made of DLSPPWs. The nominal coupling length shown here is the same as that which is varied systematically in Fig. 4. **b**, S-bends in the dielectric waveguides shift the outputs by 500 μm with respect to the inputs, ensuring that no stray light reaches the outputs. **c**, The dielectric and plasmonic waveguides were designed for optimal overlap of their modes. The colour plots show $|E|^2$ and the scale bars are 300 nm. **d**, For wavelengths shorter than 770 nm, a second mode appears in the DLSPPWs. At 814 nm, however, the DLSPPWs support only a single mode. The red line marks the effective index of the slab surface plasmon-polariton mode, which is not guided by the PMMA.

comparison with the plasmonic case (Supplementary Section 4), are plotted in Fig. 3a. Each point represents the mean and standard deviation of five measurements. Because accidental coincidence counts are negligible in our case, we attribute the deviation from unit visibility to imperfect spectral overlap of the two wave packets that carry the single photons to the coupler. The temporal width of the interference dip, a measure of the mutual coherence time of the two wave packets, is 0.12 ± 0.01 ps.

The result of the same measurement, repeated for a 50–50 coupler made from 10 μm DLSPPWs, is shown in Fig. 3b. Again, we normalize the data to allow for direct comparison to the dielectric case and to correct for drift in the alignment of our optics. We observe TPQI with a visibility of 0.932 ± 0.01, far exceeding the classical limit of 0.5, and a temporal width of 0.11 ± 0.01 ps. Both the visibility and width are identical to the dielectric case to within measurement error. We note that high visibility is consistent with the predictions of the theory of TPQI in a lossy beam splitter[23], which we extend to the case of a lossy directional coupler (Supplementary Section 1).

To provide further evidence that this measurement does in fact result from TPQI at the plasmonic coupler, we performed similar measurements in plasmonic couplers with different coupling lengths (Fig. 2a), and hence different splitting ratios. The results are shown in Fig. 4. As expected, for splitting ratios that deviate from 50–50, the visibility of TPQI reduces monotonically. Additionally, we illuminated one input of each coupler with an 800 nm alignment laser and used a digital camera with magnifying optics to form images of the light that diverged out of the outputs of the waveguides. As shown in the inset images in Fig. 4, the intensity distribution between the couplers' two outputs changes

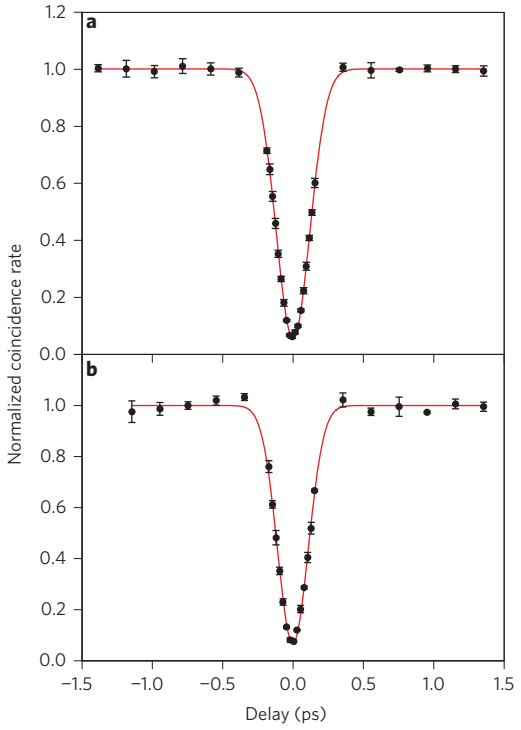

Figure 3 | Measurements of TPQI in 50–50 directional couplers. a,**b**, In the dielectric coupler (**a**) we observe TPQI with a visibility of 0.944 ± 0.003 and a temporal width of 0.12 ± 0.01 ps, while in the plasmonic case (**b**) we observe a visibility of 0.932 ± 0.01 and a width of 0.11 ± 0.01 ps. Each point represents the mean of a set of five measurements of ∼3,000 counts each (dielectric coupler) or three measurements of ∼1,600 counts each (plasmonic coupler). The red lines show fits to an inverted Gaussian function (Supplementary Section 2), from which we extracted the visibility and width of each interference dip. The error bars on individual points show ±1 s.d. of the measurements taken, while estimated errors in the visibilities, also ±1 s.d., were derived from fitting the model function to the data. The estimated error in the widths of the dips represents the precision of the adjustable delay line.

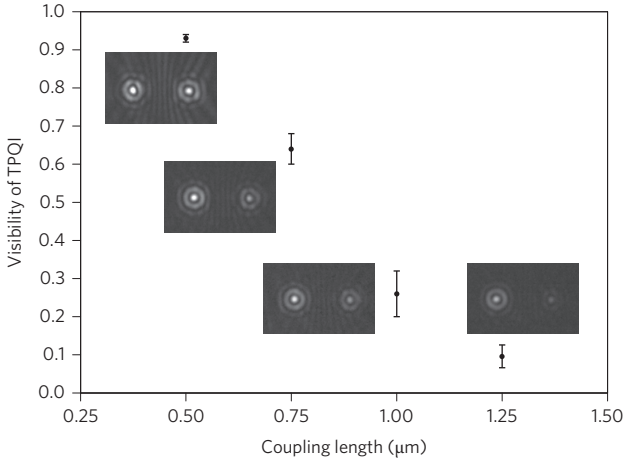

Figure 4 | TPQI in plasmonic couplers of different lengths. As expected, the visibility of TPQI decreases as the splitting ratio of the directional coupler deviates from 50–50. Insets: images showing light diverging from the outputs of the waveguides, confirming that the coupler becomes more asymmetric as the coupling length increases.

systematically with coupling length, confirming that the directional couplers are indeed functioning as intended.

We conclude that our experiment demonstrates unambiguous quantum interference in plasmonic waveguides. Moreover, the close correspondence between our measurements of TPQI in dielectric and plasmonic waveguides shows that identical photons remain indistinguishable from one another in tightly confined, high-loss plasmonic structures in which the electromagnetic fields interact strongly with the metal. This high degree of coherence confirms that plasmonic components could indeed find application in quantum computing if loss can be mitigated. Finally, by integrating plasmonic waveguides directly into a chip-based quantum photonics platform operating at room temperature, our experiment lays the groundwork for further investigations of quantum interference and entanglement in plasmonic circuits.

Methods

Two-photon source and coupling optics. We used a 100 mW, 407 nm diode laser and a bismuth borate (BiBO) crystal in our SPDC set-up. To increase the rate of photon-pair production, we inserted lenses in front of and behind the BiBO crystal which focused the laser into the crystal and collected the divergent downconverted light, respectively. A pair of identical 5 nm bandpass filters centred at 814 nm rejected background light, and two collimators collected the single photons into single-mode, polarization-maintaining fibres. Connecting these fibres to a pair of silicon SPADs, each ∼50% efficient at this wavelength, yielded ∼32,000 coincidence counts per second.

Waveguide fabrication. We started with silicon wafers on which a 3 μm wet thermal oxide layer and a 300 nm low pressure chemical vapour deposition (LPCVD) silicon nitride layer had been grown. After patterning the dielectric waveguides in ma-N 2403 negative tone resist using a 100 kV electron-beam lithography system, we transferred the pattern into the silicon nitride layer using an inductively coupled plasma reactive ion etcher. A second electron-beam lithography step defined windows in the PMMA for the gold pads. We used hydrofluoric acid to etch into the underlying SiO_2 and then deposited gold using an electron-beam evaporator. After lifting off the gold in acetone, we verified that the recessed gold pad was flush with the surface to within 10–20 nm. Two final electron-beam lithography steps defined the DLSPPWs and the PMMA spot-size converters over the tapered ends of the waveguides. Finally, we scribed the chip using a precision scribing tool and cleaved it to obtain smooth end facets.

Received 8 October 2013; accepted 29 January 2014; published online 2 March 2014

References

1. Elson, J. M. & Ritchie, R. H. Photon interactions at a rough metal surface. *Phys. Rev. B* **4,** 4129–4138 (1971).
2. Tame, M. S. *et al.* Single-photon excitation of surface plasmon polaritons. *Phys. Rev. Lett.* **101,** 190504 (2008).
3. Ballester, D., Tame, M. S. & Kim, M. S. Quantum theory of surface-plasmon polariton scattering. *Phys. Rev. A* **82,** 012325 (2010).
4. Hong, C. K., Ou, Z. Y. & Mandel, L. Measurement of subpicosecond time intervals between two photons by interference. *Phys. Rev. Lett.* **59,** 2044–2046 (1987).
5. Chang, D. E., Sørensen, A. S., Hemmer, P. R. & Lukin, M. D. Quantum optics with surface plasmons. *Phys. Rev. Lett.* **97,** 053002 (2006).
6. Akimov, A. V. *et al.* Generation of single optical plasmons in metallic nanowires coupled to quantum dots. *Nature* **450,** 402–406 (2007).
7. Kolesov, R. *et al.* Wave–particle duality of single surface plasmon polaritons. *Nature Phys.* **5,** 470–474 (2009).
8. Heeres, R. W. *et al.* On-chip single plasmon detection. *Nano Lett.* **10,** 661–664 (2010).
9. Di Martino, G. *et al.* Quantum statistics of surface plasmon polaritons in metallic stripe waveguides. *Nano Lett.* **12,** 2504–2508 (2012).
10. Altewischer, E., van Exter, M. P. & Woerdman, J. P. Plasmon-assisted transmission of entangled photons. *Nature* **418,** 304–306 (2002).
11. Fasel, S. *et al.* Energy–time entanglement preservation in plasmon-assisted light transmission. *Phys. Rev. Lett.* **94,** 110501 (2005).
12. Fasel, S., Halder, M., Gisin, N. & Zbinden, H. Quantum superposition and entanglement of mesoscopic plasmons. *New J. Phys.* **8,** 13 (2006).
13. Huck, A. *et al.* Demonstration of quadrature-squeezed surface plasmons in a gold waveguide. *Phys. Rev. Lett.* **102,** 246802 (2009).
14. Politi, A., Cryan, M. J., Rarity, J. G., Yu, S. & O'Brien, J. L. Silica-on-silicon waveguide quantum circuits. *Science* **320,** 646–649 (2008).
15. Ou, Z. Y. & Mandel, L. Derivation of reciprocity relations for a beam splitter from energy balance. *Am. J. Phys.* **57,** 66–67 (1989).

16. Ou, Z. Y., Gage, E. C., Magill, B. E. & Mandel, L. Fourth-order interference technique for determining the coherence time of a light beam. *J. Opt. Soc. Am. B* **6,** 100–103 (1989).
17. Ren, X.-F., Guo, G.-P., Huang, Y.-F., Wang, Z.-W. & Guo, G.-C. Plasmon assisted transmission of single photon wavepacket. *Metamaterials* **1,** 106–109 (2007).
18. Wang, S. M. *et al.* Hong–Ou–Mandel interference mediated by the magnetic plasmon waves in a three-dimensional optical metamaterial. *Opt. Express* **20,** 5213–5218 (2012).
19. Fujii, G. *et al.* Preservation of photon indistinguishability after transmission through surface-plasmon-polariton waveguide. *Opt. Lett.* **37,** 1535–1537 (2012).
20. Heeres, R. W., Kouwenhoven, L. P. & Zwiller, V. Quantum interference in plasmonic circuits. *Nature Nanotech.* **8,** 719–722 (2013).
21. Shoji, T., Tsuchizawa, T., Watanabe, T., Yamada, K. & Morita, H. Low loss mode size converter from 0.3 μm square Si wire waveguides to singlemode fibres. *Electron. Lett.* **38,** 1669–1670 (2002).
22. Briggs, R. M., Grandidier, J., Burgos, S. P., Feigenbaum, E. & Atwater, H. A. Efficient coupling between dielectric-loaded plasmonic and silicon photonic waveguides. *Nano Lett.* **10,** 4851–4857 (2010).
23. Barnett, S. M., Jeffers, J., Gatti, A. & Loudon, R. Quantum optics of lossy beam splitters. *Phys. Rev. A* **57,** 2134–2145 (1998).

Acknowledgements

This work was supported by the Air Force Office of Scientific Research under MURI awards FA9550-12-1-0488 (J.S.F.), FA9550-12-1-0024 (H.L.) and FA9550-04-1-0434 (Y.A.K.). The authors thank the Kavli Nanoscience Institute at Caltech for access to and maintenance of fabrication equipment. Additionally, J.S.F. would like to thank R.M. Briggs for fabrication training and advice.

Author contributions

J.S.F. and H.A.A. designed the experiment. J.S.F. and Y.A.K. built and tested the SPDC source. J.S.F. and H.L. built and tested the waveguide-coupling set-up. J.S.F. fabricated the waveguides. H.L. performed the measurements of quantum interference. All authors contributed to writing the manuscript.

Additional information

Supplementary information is available in the online version of the paper. Reprints and permissions information is available online at www.nature.com/reprints. Correspondence and requests for materials should be addressed to H.A.A.

Competing financial interests

The authors declare no competing financial interests.